Segmented Electrode Losses In MHD Generators With Nonequilibrium Ionization - Ii

Author(s): Jack L. Kerrebrock

Session Name: All

SEAM: 6 (1965)

SEAM EDX URL: https://edx.netl.doe.gov/dataset/seam-6

EDX Paper ID: 133

SEGMENTED ELECTRODE LOSSES IN MHD GENERATORS WITH NONEQUILIBRIUM IONIZATION - II

Jack L. Kerrebrock
Consultant to Avco-Everett Research Laboratory, Everett, Mass., and
Associate Professor, Dept. of Aeronautics and Astronautics, M.I.T., Cambridge, Mass.

Abstract

In MHD generators designed to produce nonequilibrium ionization by electron heating, the electrical conductivity may be very high near segmented electrode walls, where the concentrated dissipation produced by blockage of the conduction current at the surface of the insulator may produce much higher electron temperatures than exist in the bulk of the gas. The nonuniform conductivity tends to cause Hall current shorts which increase the dissipation and the conductivity near the electrodes. The effect of this phenomenon on the performance of segmented electrode generators is analyzed, with the principal aim of predicting the electron temperature rise in such devices. One conclusion of the analysis is that generators with rather coarse segmentation are less subject to this type of loss than are generators with very fine segmentation, and will therefore yield larger electron temperatures. A second conclusion is that, to maximize the electron temperature rise, operation at high Mach number, but rather low Hall parameter, is desirable. While there is not sufficient experimental data to properly verify these conclusions, the available data is at least consistent with them.

I. Introduction

As the title of this article indicates, it is concerned with the losses which occur near the segmented electrodes in MHD generators designed to produce nonequilibrium ionization by electron heating. The first clear evidence that electrode losses in such generators are qualitatively different from those in equilibrium generators, was provided by the failure of the segmented electrode generator of Klepeis and Rosa[1] to produce the expected Hall voltages. Attempts to correlate the observed Hall voltages with the predictions of the electrode theory of Hurwitz, Kilb and Sutton[2] showed that the losses were much larger than the theory predicted.

An explanation for these large losses was offered in Ref. 3 where it was proposed that the Ohmic dissipation near the electrodes results in elevation of the electron temperature, and conductivity, above their respective free stream values. The resulting nonuniformity was found to lead to the flow of local Hall currents, which would further increase the local dissipation and hence the conductivity. Such a nonuniformity would therefore tend to be self-supporting.

An approximate theory of generator performance, based upon these ideas was given in Ref. 3. It predicted even lower performance than was observed by Klepeis and Rosa,[1] but this was acceptable since the theory was expected to give an upper limit to the losses.

This theory was however subject to two principal criticisms. First, it was assumed in computing the elevation of electron temperature near the electrodes, that the electrons lost energy only by elastic collisions, and the energy loss coefficient was adjusted to account for other losses. We know that energy loss by resonance radiation crucially influences the electronic energy balance,[4,5] and that this loss cannot be represented properly by an effective energy loss coefficient. Secondly, the theory was so complicated (numerically) that it was difficult to draw general conclusions.

Both of these deficiencies have been corrected in the modified theory to be presented here. The radiant energy loss is computed locally, using the resonance escape probability of Holstein[6] with the result that the theory now contains no empirical factors.

The results suggest the rather surprising conclusion that a nonequilibrium generator is more likely to succeed with rather coarse electrode segmentation than with fine segmentation.

There is at present very little data with which to compare the theory. Apart from the early experiment of Robben,[7] there are only the data of Klepeis and Rosa[1] and of Croitoru, Bekiarian, Graziotti, and Pithon,[8] although other investigators have reported failure of nonequilibrium generators to achieve the expected performance.[9,10]

Scanty as they are, these data appear to confirm the results of the analysis, which is therefore offered as a guide to the design of successful nonequilibrium generators.

II. Distribution of Electron Heating

Before beginning a detailed calculation of the electrode losses in a nonequilibrium generator, it will be well to consider the basic cause of the losses.

We note first that the distribution of current density is given approximately by the generalized Ohm's law,

$$\vec{j} = \sigma \vec{E}' - \beta \frac{\vec{j} \times \vec{B}}{B} \tag{1}$$

where σ is the scalar conductivity, β is the Hall parameter, and $\vec{E}' = \vec{E} + \vec{u} \times \vec{B}$ is the electric field measured in the fluid.

The conductivity is related to the current density, or to the Ohmic heating rate, j^2/σ, by an expression of the form,

$$\frac{j^2}{\sigma} = \vec{j} \cdot \vec{E}' = \delta_e \frac{m_e}{m_a} n_e \nu_c \frac{3}{2} k (T_e - T_a) + Q_r \tag{2}$$

where the first term represents the elastic collisional energy loss, and Q_r represents the radiant energy loss. Increasing j^2/σ increases T_e, which in turn increases σ.

Referring now to Eq. (1) and to Fig.1, which schematically depicts a segmented generator channel, we note that at a point near the insulating segment of the wall, $j_y = 0$, and $j_x = \sigma_i E_{xi}$, the subscript "i" denoting the surface of the insulator. In the free stream, if the generator operates in the Faraday mode, $j_x = 0$, and $j_y = \sigma_\infty E'_{y\infty}$. Furthermore, in the free stream, $E_{x\infty} = \beta_\infty E'_{y\infty}$, and if the channel length is large compared to its height (2H), $E_{xi} \geq E_{x\infty}$.

It therefore follows that

$$\frac{(\vec{j} \cdot \vec{E}')_i}{(\vec{j} \cdot \vec{E}')_\infty} = \frac{\sigma_i E_{xi}^2}{\sigma_\infty E_{x\infty}^2} = \frac{\sigma_i}{\sigma_\infty} \beta_\infty^2 \tag{3}$$

From Eq. (2), we see that if Q_r is [s]mall $T_e - T_a \propto \vec{j} \cdot \vec{E}'$ and would therefore [b]e much larger near the insulator than in [th]e free stream. This could cause σ_i/σ_∞ [t]o be greater than unity, which would further increase $T_e - T_a$ near the wall. The net result is that in a generator designed to produce nonequilibrium ionization, the electron heating is much more likely to occur near the electrodes than in the free stream.

This conclusion must be modified slightly because Q_r is much larger near the wall than in the free stream. We shall assume in the present analysis that Q_r is locally equal to the energy loss for a transparent gas, multiplied by the local resonance escape probability. Then Q_r may be written,

$$Q_r = \frac{2\pi e^2 n_0 h \nu_0^3}{m_e c^3 \epsilon_0} e^{-\frac{h\nu_0}{kT_e}} \sum_i \alpha_i g_i f_{i\to 0} \tag{4}$$

where n_0 is the density of seed atoms in the ground state, ν_0 is the frequency of the resonance line (or an average frequency for the doublet in the alkali metals), α_i is the resonance escape probability for the i^{th} line, while $g_i f_{i\to 0}$ is the product of degeneracy and emission oscillator strength for the line. Values for $g_i f_{i\to 0}$ are given in Ref. 11.

For the case of dispersion (pressure) broadening, Holstein,[6] gives the result

$$\alpha_i(y) = \left(\frac{2 g_0 \gamma_p \nu_i^2}{c^2 n_0 g_i \gamma y} \right)^{1/2} \tag{5}$$

where γ and γ_p are the natural and total line widths, and y is the distance of the point in question from the (absorbing) boundary of the plasma.

In choosing this form for Q_r we have implicitly assumed that the radiation always removes energy from the electrons, whereas it can in fact either add to or subtract from their energy, depending on whether the radiant energy flux is greater than or less than the local equilibrium flux.

However, our principal interest is in the situation where the electron temperature is higher near the wall than elsewhere, and in this case the assumption is at least qualitatively correct.

For a typical mixture of noble gas and alkali metal, $\alpha \approx 10^{-3}$ for $y \approx 1$ cm, so that in the bulk of the gas, Q_r is much less than it would be for a transparent gas. At the surface, $\alpha = 1$, and Q_r is so large that the electron temperature must be depressed there to a value near (or below) the wall temperature. But if within a length of the order of L from the wall, $\alpha(y)$ becomes small, the radiant energy loss becomes of the same order as the elastic energy loss, and a layer of highly conducting gas can form.

If L is sufficiently small, the radiation will depress the electron temperature and prevent the formation of the layer of highly conducting fluid. However, as we shall see, this should occur only if L is a small fraction of a millimeter.

For the present purposes it will be convenient to refer Q_r to the corresponding value in the main flow. Thus,

$$\frac{Q_r}{Q_{r\infty}} \approx \left(\frac{H}{y}\right)^{1/2} e^{-\frac{h\nu_0}{kT_{e\infty}}\left(\frac{T_{e\infty}}{T_e} - 1\right)} \tag{6}$$

where we are neglecting the variations of n_0 and γ_p in comparison to those of (y/H) and the exponential. Also for the sake of convenience, we shall define an effective δ_∞ for the main flow through Eq. (2) as

$$\delta_\infty \equiv \frac{(\vec{j} \cdot \vec{E}')_\infty}{\frac{m_e}{m_a} n_{e\infty} \nu_{c\infty} \frac{3}{2} k (T_{e\infty} - T_{a\infty})} \tag{7}$$

The magnitude of δ_∞ is then calculable by use of Eqs. (2), (4), and (5). In fact, we see that since δ_∞ depends on H, we may take δ_∞, or the ratio δ_∞/δ_e as a measure of the generator size.

III. Approximate Formulation

The essential elements of the desired theory are, first a method for computing the current distribution due to electrode segmentation for a nonuniform gas, and secondly, a method for relating the state of the gas to the (dissipative) losses. It is clearly impractical to attempt an exact solution, in which the local properties of the gas are determined by the local dissipation. Rather, we shall adopt an integral approach in which a profile for electron temperature is assumed, the losses are calculated, and then a form of Eq. (2) which has been integrated in y is satisfied.

A. Current Distribution

Consider a slightly ionized plasma in steady flow through a channel having the configuration sketched in Fig. 1. The flow of currents within the plasma will be governed by Eq. (1), subject to the conditions:

$$\nabla \times \vec{E} = 0$$

and

$$\nabla \cdot \vec{J} = 0$$

Combining these relations, we obtain a general equation for the current:

$$\frac{1}{\sigma}\nabla\times\vec{J} + \nabla\left(\frac{1}{\sigma}\right)\times\vec{J} + \frac{\beta}{B\sigma}\left[(\vec{B}\cdot\nabla)\vec{J} - (\vec{J}\cdot\nabla)\vec{B}\right] + \nabla\left(\frac{\beta}{B\sigma}\right)\times(\vec{J}\times\vec{B}) + \vec{B}(\nabla\cdot\vec{u}) - \vec{B}\cdot\nabla(\vec{u}) + (\vec{u}\cdot\nabla)\vec{B} = 0 \quad (8)$$

We will assume that $\vec{B} = B_z$ is uniform and normal to both $\nabla\vec{J}$ and $\nabla\vec{u}$, and that $\vec{B}(\nabla\cdot\vec{u})$ may be neglected. Somewhat less confidently, we assume that $\sigma = \sigma(y)$ and $\beta = \beta(y)$, because convection should tend to maintain uniformity in the x (streamwise) direction. It is difficult to prove that this assumption is valid, because very large concentrations of current may develop, and these could induce sharp variations in the x direction. Nevertheless, it seems consistent with the present integral formulation to average these variations in x.

Defining a "stream function" ψ such that

$$j_x = -\frac{\partial\psi}{\partial y} \qquad j_y = \frac{\partial\psi}{\partial x} \quad (9)$$

we find that Eq. (8) becomes,

$$\frac{\partial^2\psi}{\partial x^2} + \frac{\partial^2\psi}{\partial y^2} - \left(\frac{\partial\psi}{\partial y} + \beta\frac{\partial\psi}{\partial x}\right)\frac{d\log\sigma}{dy} + \left(\frac{\partial\psi}{\partial x}\right)\frac{d\beta}{dy} = 0 \quad (10)$$

Now if we assume that the electron temperature and the gas temperature both vary linearly with y in a region of height h near the electrode surface, then both $d\beta/dy$ and $d\log\sigma/dy$ will be nearly constants. We denote them as ν and μ respectively, and note that, for a slightly ionized gas,

$$\frac{\beta}{\beta_\infty} = 1 + \frac{\mu}{\beta_\infty}(y-H) \; ; \quad H < y < H+h \quad (11)$$

and

$$\frac{n_e}{n_{e\infty}} = \frac{e^{\nu(y-H)}}{1 + \frac{\mu}{\beta_\infty}(y-H)} \approx e^{-\lambda\left(\frac{T_{e\infty}}{T_e}-1\right)} \; ; \quad H < y < H+h \quad (12)$$

where $\lambda = \epsilon_i/2kT_{e\infty}$ if ϵ_i is the ionization energy of the seed material. For complete consistency, the Hall parameter should be treated as a variable in the third term of Eq. (10), but to reduce the equation to one with constant coefficients, we shall assume that this β is $\bar{\beta} = \beta_\infty + \mu h/2$. The equation is then finally:

$$\frac{\partial^2\psi}{\partial x^2} + \frac{\partial^2\psi}{\partial y^2} - \nu\frac{\partial\psi}{\partial y} + (\mu - \bar{\beta}\nu)\frac{\partial\psi}{\partial x} = 0 \quad (13)$$

There is some difficulty in selecting appropriate boundary conditions for this equation. Hurwitz, Kilb and Sutton[2] computed the current distribution for $\mu = \nu = 0$, imposing boundary conditions such that $j_y = 0$ on the insulators and $E_x = 0$ on the electrodes. Their results indicate singular concentrations of current at the edges of the electrodes. These very sharp concentrations result from the condition $E_x = 0$ and since the large current concentrations would in reality lead to sizeable electric fields in the electrodes, they do not seem to be completely realistic.

Partially for this reason, and partially for ease in computation, we shall specify boundary conditions on the normal current, j_y, at the electrodes rather than on E_x. In fact we shall assume that the total current J per electrode is uniformly distributed over the electrode width $2l$.

Again for the sake of simplicity, we shall eliminate the problem of matching the wall regions to the main flow by computing the currents in a single region of height $2h$, and then separating its halves by the uniform region of height $2H$. Thus defining $y' = y - H$, the boundary conditions are:

$$j_y(h) = j_y(-h) = \frac{J}{2l} \; ; \; -l < x < l$$

$$j_y(h) = j_y(-h) = 0 \; ; \; -L < x < l \; ; \; l < x < L$$

The solution can be obtained by a straightforward series expansion. Putting

$$\psi = \frac{a_0}{2} x + \sum_{n=1}^{\infty} \left[\frac{a_n(y')}{k_n} \sin k_n x - \frac{b_n(y')}{k_n} \cos k_n x \right] + A(y') \tag{14}$$

where $k_n = n\pi/L$, we find

$$a_0 = J/L \tag{15}$$

$$\frac{dA}{dy'} = -\frac{J}{2L}\left(\bar{\beta} - \frac{\mu}{\nu}\right) + C e^{\nu y'} \tag{16}$$

The results for a_n and b_n are quite complicated in general, but for $k_n h$ large, they become

$$a_n \sim \frac{2J}{n\pi l} \sin \frac{n\pi l}{L} \left(\frac{2\mu_n \lambda_n k_n}{\bar{\beta}\nu - \mu} \right) e^{-\frac{\nu h}{2} - \lambda_n k_n h + \frac{\nu y'}{2}} \Big\{ \sin \mu_n k_n h \cosh \lambda_n k_n y \cos \mu_n k_n y + \sin \mu_n k_n h \sinh \lambda_n k_n y \sin \mu_n k_n y \Big\} \tag{17}$$

$$b_n \sim -\frac{2J}{n\pi l} \sin \frac{n\pi l}{L} \left(\frac{2\mu_n \lambda_n k_n}{\bar{\beta}\nu - \mu} \right) e^{-\frac{\nu h}{2} - \lambda_n k_n h + \frac{\nu y'}{2}} \Big\{ \sin \mu_n k_n h \cosh \lambda_n k_n y \cos \mu_n k_n y + \cos \mu_n k_n h \sinh \lambda_n k_n y \cos \mu_n k_n y \Big\} \tag{18}$$

where

$$\lambda_n = \frac{1}{\sqrt{2}} \left\{ \left[\left(1 + \frac{\nu^2}{4k_n^2} \right)^2 + \left(\frac{\bar{\beta}\nu - \mu}{k_n} \right)^2 \right]^{1/2} + 1 + \frac{\nu^2}{4k_n^2} \right\}^{1/2}$$

$$\mu_n = \frac{1}{\sqrt{2}} \left\{ \left[\left(1 + \frac{\nu^2}{4k_n^2} \right)^2 + \left(\frac{\bar{\beta}\nu - \mu}{k_n} \right)^2 \right]^{1/2} - 1 - \frac{\nu^2}{4k_n^2} \right\}^{1/2}$$

Because $k_n h = n\pi h/L > 1$ these approximations are adequate.

Except for the determination of C the solution for J is complete. From Eqs. (9), (14), (15), (16), (17), $\vec{J}$ can be calculated if ν is prescribed.

B. Performance Characteristics

We define the voltages between electrodes in the x and y directions by

$$V_x = \int_0^{2L} E_x(x, h)\, dx$$

$$V_y = 2 \int_0^{H+h} E_y(0, y)\, dy$$

and the net Hall current by

$$J_H = 2 \int_0^{H+h} j_x(L, y)\, dy$$

Then using Eq. (1) in the form,

$$\vec{E} = \frac{\vec{J}}{\sigma} + \left(\frac{\beta}{\sigma}\right) \vec{J} \times \vec{B} + \vec{u} \times \vec{B}$$

and Eqs. (14) and (17) for $\vec{J}$, we can determine the relations between the overall voltages and total currents in the x and y directions.

It is convenient to define another parameter,

$$J_{ideal} = \sigma_\infty \frac{L}{H+h}\left[V_y - 2u_\infty B(H+h)\right] \qquad (19)$$

which is the current per electrode in an ideal generator with the actual free stream conductivity.

We then find the following relation:

$$\frac{J}{J_{ideal}} = \frac{1 + \frac{h}{H+h}\left(\frac{1-\bar{u}/u_\infty}{K-1}\right) - \frac{L}{h}\left[\frac{\beta_\infty\left(1+\frac{\mu h}{2\beta_\infty}\right)}{\frac{e^{\nu h}-1}{\nu h}+\frac{H}{h}}\right]\frac{J_H}{J_{ideal}}}{\left\{\begin{array}{l}(1+\beta_\infty^2)\frac{h}{H+h}\left[\frac{1-e^{-\nu h}}{\nu h}+\frac{H}{h}\right]-\beta_\infty^2\left[\frac{H+h}{h}+\frac{\mu h}{2\beta_\infty}\right]\left[1+\frac{\mu h}{2\beta_\infty}\left(\frac{h}{H+h}\right)\left(1+\frac{1-e^{-\nu h}}{\nu h}\right)\right]\Big/\left[\frac{e^{\nu h}-1}{\nu h}+\frac{H}{h}\right] \\ +\beta_\infty^2\left(\frac{\mu h}{2\beta_\infty}\right)\left(\frac{h}{H+h}\right)\left\{\frac{1-e^{-\nu h}}{\nu h}+\left(1+\frac{\mu h}{2\beta_\infty}\right)\left[e^{-\nu h}+\frac{2}{\nu h}\,\frac{1-(1+\nu h)e^{-\nu h}}{\nu h}\right]\right\}+2\frac{L}{H+h}e^{-\nu h}\sum'\end{array}\right\}}$$

where the indicated sum is

$$\sum' = \sum_{n=1}^{\infty}\frac{L}{2n\pi}\sin\frac{n\pi l}{L}\left\{\frac{(2n\pi\lambda_n-\nu L)+4n\pi\lambda_n\mu_n^2\left[\frac{\beta_\infty\nu+\mu(\nu h-1)}{\nu\left(\beta_\infty+\frac{\mu h}{2}\right)-\mu}\right]}{(n\pi\lambda_n-\nu L/2)^2+(n\pi\mu_n)^2}\right\} \qquad (21)$$

The quantity $\bar{u}$ is the mean flow velocity in the region of height h, while K is the loading parameter, i.e., $K=V_y/2u_\infty B(H+h)$.

A similar relation is obtained for the actual Hall voltage V_x, per electrode, divided by the ideal Hall voltage:

$$\frac{\sigma_\infty V_x}{-\beta_\infty J_{ideal}} = \frac{\left\{\frac{H+h}{h}+\frac{\mu h}{2\beta_\infty}\left[1+\frac{1-e^{-\nu h}}{\nu h}\right]\right\}\frac{J}{J_{ideal}} - \frac{L}{h}\,\frac{J_H}{\beta_\infty J_{ideal}}}{\left[\frac{e^{\nu h}-1}{\nu h}+\frac{H}{h}\right]} \qquad (22)$$

In addition to these parameters, we wish to know the electron temperature in the main flow. Since the currents and electric fields are known, it can be found from Eq. (2). The result is that

$$\frac{\frac{T_{e\infty}}{T_{a\infty}}-1}{\left(\frac{T_e}{T_a}-1\right)_{ideal}} = \frac{\delta_e}{\delta_\infty}\left\{\left(\frac{J}{J_{ideal}}\right)^2 + \beta_\infty^2\left[\frac{J}{J_{ideal}} - \frac{\left\{\frac{H+h}{h}+\frac{\mu h}{2\beta_\infty}\left[1+\frac{1-e^{-\nu h}}{\nu h}\right]\right\}\frac{J}{J_{ideal}} - \frac{L}{h}\frac{J_H}{\beta_\infty J_{ideal}}}{\left[\frac{e^{\nu h}-1}{\nu h}+\frac{H}{h}\right]}\right]^2\right\} \quad (23)$$

where the ideal electron temperature rise, $(T_e/T_a-1)_{ideal}$ is defined by

$$\left(\frac{T_e}{T_a}-1\right)_{ideal} = \frac{2\gamma}{3\delta_e} M_\infty^2 \beta_\infty^2 (1-K)^2 \quad (24)$$

Here $\gamma = C_p/C_v$ and M_∞ is the flow Mach number.

These relations completely specify the performance of the generator if ν and h are given. Some typical results are shown in Figs. 2,3,4 for a case where the wall temperature equals the gas temperature ($\mu h/\beta_\infty = 0$), where there is no velocity boundary layer ($\bar{u}/u_\infty = 1$), and where $J_H = 0$. The value of $\delta_\infty/\delta_e = 5$ is appropriate to a channel having a least dimension of the order of 1 cm if the seed density is of the order of 10^{16} cm^{-3}.

It will be noted that reductions and increases in the conductivity near the electrode are about equally damaging to the performance. Perhaps the most striking feature of these results is the great reduction in the electron temperature increment which is caused by even small values of νh for large β_∞.

The effect of a reduction in wall temperature is indicated in Fig. 5 which is drawn for $\mu h/\beta_\infty = -.5$, i.e., for a wall temperature equal to one-half the gas temperature. In this case the performance is greatly improved for $\nu h < 0$, over that for the "hot wall".

C. Determination of νh:

These results are incomplete in that ν and h remain to be determined. As noted above, we shall determine them by requiring that the total dissipation in the layer of fluid of height h be that required to support the excess of electron temperature implied by the assumed values of ν and h.

In Ref. 3 where radiant energy losses were not included, an additional condition was imposed, namely that the electron temperature at the surface should be that implied by Eqs. (2) and (3). Thus, both ν and h were determined independently. This second condition cannot be applied when radiation is accounted for. The radiation depresses T_e very near the surface, giving a profile which is too complicated to be represented by a linear approximation.

We must therefore abandon the surface condition, and replace it by a further assumption regarding the electron temperature profile. Trial calculations have indicated that the results are quite insensitive to the magnitude of h, so it will be assumed that $h/L = 1$.

The value of νh is then determined by the condition that the integral of Eq. (2) over the layer of height h, be satisfied. That is

$$\int_0^h (\vec{J}\cdot\vec{E}')\,dy = \int_0^h\left\{\delta_e \frac{m_e}{m_a} n_e \nu_c \frac{3}{2}k(T_e-T_a) + Q_r(y)\right\}dy \quad (25)$$

It would be quite difficult to determine the left integral from the solutions for $\vec{J}$ and $\vec{E}'$, but fortunately it can be determined from the overall characteristics. We know that the losses in the generator must all appear as Ohmic heating of the gas, and the overall losses can be computed from J, V_y, and the ideal voltage. Thus, if we let the excess dissipation per electrode pair (over that in the free stream) be denoted D, it follows that

$$D = -J\left[2(H+h)U_\infty B - V_y\right] - 4L(H+h)\delta_\infty \frac{m_e}{m_a} n_{e\infty} \nu_{c\infty} \frac{3}{2}k\,(T_{e\infty} - T_{a\infty})$$

$$= 2\int_0^h \left[\vec{J}\cdot\vec{E}' - (\vec{J}\cdot\vec{E}')_\infty\right] dy$$

The right hand integral in Eq. (25) can be evaluated, using the assumed form for $T_e(y)$, which is $T_e/T_{e\infty} = 1/(1-\nu y/\lambda)$; $H < y < H+h$. The corresponding forms for n_e and β are given by Eqs. (11) and (12).

With some manipulation, Eq. (25) can then be written in the following form:

$$\left(\frac{T_e}{T_a}-1\right)_{ideal} = \frac{I_1 - I_2}{\frac{H+h}{h}\left(\frac{J}{J_{ideal}}\right) - \left\{\frac{\delta_\infty}{\delta_e}\frac{H}{h} + I_1 + \frac{\delta_\infty - \delta_e}{\delta_e}\left(\frac{H}{h}\right)^{1/2} I_3\right\}\frac{T_{e\infty}/T_{a\infty}-1}{(T_e/T_a-1)_{ideal}}} \tag{26}$$

where

$$I_1 = \int_0^1 \frac{e^{\nu h \xi'}\, d\xi'}{\left(1-\frac{\nu h}{\lambda}\xi'\right)^2\left(1+\frac{\mu h}{\lambda}\xi'\right)^2}$$

$$I_2 = \int_0^1 \frac{e^{\nu h \xi'}\, d\xi'}{\left(1-\frac{\nu h}{\lambda}\xi'\right)\left(1+\frac{\mu h}{\lambda}\xi'\right)}$$

$$I_3 = \frac{2e^{2\frac{\epsilon_e}{\epsilon_i}\nu h}}{1+\frac{\mu h}{\beta_\infty}} - 2\int_0^1 \left\{\frac{2\frac{\epsilon_e}{\epsilon_i}\nu h\left(1+\frac{\mu h}{\beta_\infty}\xi'\right) - \frac{\mu h}{\beta_\infty}}{\left(1+\frac{\mu h}{\beta_\infty}\xi'\right)^2}\right\} e^{2\frac{\epsilon_e}{\epsilon_i}\nu h \xi'}\, \xi'^{1/2}\, d\xi'$$

and ϵ_e is the energy of the first excited state of the seed atom.

This equation may be regarded as a determination of νh in terms of $(T_e/T_a-1)_{ideal}$, which is a design parameter for the generator. The calculation is therefore completely closed. To recapitulate, the generator design is specified by the dimensions H, L, and ℓ. The gas properties are determined by M_∞, β_∞, $T_{a\infty}$ and $\mu h/\beta_\infty$ plus the usual cross sections, etc. We assume $h/L = 1$. Then if we specify the loading, K, $(T_e/T_a-1)_{ideal}$ is determined. Now if we specify the Hall current, J_H, Eqs. (7), (20), (22), (23), and (25) can be solved for νh, δ_∞/δ_e and the three performance parameters, J/J_{ideal}, $\sigma_\infty V_x/-\beta_\infty J_{ideal}$, and $(T_{e\infty}/T_{a\infty}-1)/(T_e/T_a-1)_{ideal}$

In practice, it has proven easiest to specify β_∞, νh, H/L, ℓ/L, $\mu h/\beta_\infty$, δ_∞/δ_e and J_H/J_{ideal} and compute the performance variables and directly. The performance variables can then be plotted as functions of $(T_e/T_a-1)_{ideal}$, β_∞, H/L, ℓ/L, $\mu h/\beta_\infty$, J_H/J_{ideal}, and δ_∞/δ_e. The results will be given in this form in the next section.

IV. Theoretical Results

Calculations have been carried out for quite a wide range of parameters. It will be possible to display only a small fraction of the results here. The results which will be given have been chosen to display the major trends and to permit comparison with experiments where they are available.

A. The Stability Boundary

The most important result of the analysis is illustrated in Fig.6, which gives the predicted variation of the ratio of actual and ideal electron temperature rises as a function of β_∞ and $(T_e/T_a-1)_{ideal}$, for parameters appropriate to the generator of Klepeis and Rosa.

The most significant result is that two modes of generator operation exist. One mode, which we may term the "normal" mode exists for small values of $(T_e/T_a - 1)_{ideal}$. In this mode, νh is small, and the generator realizes a large fraction of its ideal performance. A second mode, which we may term the "shorted" mode exists for large $(T_e/T_a - 1)_{ideal}$. In this mode, νh is large, there are large losses near the electrodes, and the generator realizes only a small fraction of its ideal performance. For a given β_∞, there is a value of $(T_e/T_a - 1)_{ideal}$ below which only the "normal" mode exists. Above this value both modes are possible, but it seems reasonable that the generator would select the shorted mode, which produces much greater dissipation.

Thus, in terms of $(T_e/T_a - 1)_{ideal}$, there is a stable range and an unstable range of generator operation. The actual electron temperature rise is proportional to the product of the abscissa and the ordinate, and a little arithmetic shows that the maximum of $(T_{e\infty}/T_{a\infty} - 1)$ occurs on the "normal" branch just at the stability limit. We see from Fig. 6 that the stability limit moves to the left as β_∞ increases. Thus it follows that the maximum electron temperature rise decreases as β_∞ increases, for a given generator design. This trend is shown by the upper curve in Fig. 7, where it is assumed, as in Fig. 6, that the wall temperature is one-half the free stream gas temperature.

It will be noted that in the "normal" mode the performance improves as $(T_e/T_a - 1)_{ideal}$ increases. This is because the increased dissipation near the wall raises the electron temperature there and so reduces the loss due to the cool wall. In the shorted mode the electron temperature near the wall becomes greater than the free stream temperature, and the losses are very large.

Both of the other performance parameters show trends similar to that of the electron temperature rise. The ratio of actual to ideal Hall voltages is displayed in Fig. 8 for the conditions specified in Fig. 6. To clarify the relationship between the actual electron temperature rise and the operating variables of the generator, curves of constant $(T_{e\infty}/T_{a\infty} - 1)$ are plotted versus $M_\infty(1-K)$ and β_∞ Fig.9, again for the parameters specified in Fig. 6. The stability boundary is indicated as a dashed line. To the right of and above it, the generator is "shorted". To the left of and below it, the operation is "normal". We see that for this channel design, the largest electron temperature rise should have been achieved for $\beta_\infty < 4$ and for rather high Mach numbers. As we have noted above, it was always operated in the unstable region. The operating line is indicated by the horizontal arrow.

B. The Effect of Wall Temperature

If the wall temperature is increased, the stability boundary moves to the left, since then the dissipation more readily produces a conductivity excess near the wall. This is shown in Fig. 10, which is drawn for $T_w = T_a$, or $\mu h/\beta_\infty = 0$. Further, the performance in the "normal" mode decreases as $(T_e/T_a - 1)_{ideal}$ increases, since now any dissipation near the wall makes $\nu h > 0$ and increases the losses (See Fig. 4).

The maximum $(T_{e\infty}/T_{a\infty} - 1)$ is given for this case also in Fig. 7. It is substantially less than that for the cooled wall. We therefore tentatively conclude that wall cooling should be beneficial in nonequilibrium generators, though of course this conclusion must be tempered by the realization that very cold electrodes will not emit properly.

C. Fineness of Electrode Segmentation

The effect of increasing H/L on the electron temperature is shown in Fig. 11. Here δ_∞/δ_e has been held constant at 5 so that, to the extent that a constant value of δ_∞ implies a constant channel size, the variation of H/L implies a variation of L, holding H, and other parameters constant.

For values of H/L less than about 50, and for $\mu h/\beta_\infty = -0.5$, the performance on the "normal" branch improves as H/L is increased, but the stability boundary moves to the left with the result that the maximum attainable $(T_{e\infty}/T_{a\infty} - 1)$ decreases.

For values of H/L greater than about 50, and again for $\mu h/\beta_\infty = -0.5$, the performance in the normal mode is very low because the dissipation is not large enough to elevate the conductivity near the wall. The best performance is then obtained in the "shorted" mode, but just at the stability boundary.

By raising the wall temperature, the performance in the "normal" mode can be raised, but then the stability limit moves left with the net result being a reduction of $(T_{e\infty}/T_{a\infty} - 1)_{max}$. This is shown in Fig. 11 for $H/L = 1000$.

The maximum attainable values of $T_{e\infty}/T_{a\infty} - 1$ are summarized in Fig. 12 for $\beta_\infty = 10$. We see that unless the segmentation can be almost on a molecular scale, the best choice is a rather coarse segmentation. No calculations have been done for values of H/L below 4 because it is felt that the model, which assumes thin dissipative layers near the electrodes, is not applicable for $H/L < 4$. However, there must be an optimum H/L between 0 and 4 since for $H/L = 0$, we have the case of continuous electrodes.

D. Generator Size

It was noted above that the generator size is principally reflected in δ_∞/δ_e. Figure 13 shows for $H/L = 100$, that as δ_∞/δ_e is reduced, the performance in the "normal" mode improves, but the stability limit moves to the left. The net result is a slight increase in $(T_{e\infty}/T_{a\infty}-1)_{max}$ as the generator size is increased. These maxima are tabulated with the channel dimensions implied by the values of δ_∞/δ_e, assuming that the seed mole fraction is about 0.001.

V. Comparison with Experiments

There appear to be only two sets of data which are suitable for comparison with the theory. Klepeis and Rosa[1] reported systematic measurements of Hall voltage in a segmented channel under conditions conducive to electron heating. Much more recently Croitoru, Bekiarian, Graziotti and Pithon[8] have reported measurements of load current in a segmented channel with similar conditions. We shall compare the predictions of the theory with the results of both experiments.

A. Comparison with Data of Klepeis and Rosa

For this generator, $H/L = 23$, $\delta_\infty/\delta_e = 5$, and $M_\infty \approx 0.5$. It was operated with $K = 0$ for values of β_∞ from about 4 to 15. Referring to Fig. 6 where this load line is indicated, we see that the operation was always in the unstable region. This is also indicated in Fig. 9 where the load line is indicated by the horizontal arrow.

The ratios of actual to ideal Hall voltage obtained from Fig. 7 are compared to Klepeis and Rosa's data in Fig. 14. This is the curve for $T_w/T_{a\infty} = 0.5$. Curves for $T_w/T_{a\infty} = 0.25$ and 1.0 are also shown since the actual wall temperature was not determined. The result given in Ref. 3 is also presented for comparison. We note that it is not very different from that obtained from the present analysis. Thus it appears that the results are rather insensitive to the details of the model used for the dissipative layer. This is encouraging.

On the other hand, the actual performance is considerably better than the predicted performance. No firm explanation can be offered at present. However, we may note that this generator operated with such a low gas temperature (1750°K) that the electron density was below the limit for applicability of the simple two temperature conduction law.[12] In Ref. 12 it was noted that for $n_e < 3 \times 10^{12}$ cm^{-3}, σ is much less sensitive to j than the simple theory would predict. This would tend to reduce the value of νh, and hence the losses.

B. Comparison with Data of Croitoru et al.

For this generator, $H/L = 3$, $\beta_\infty = 20$, $M_\infty = 0.57$, $T_{a\infty} = 2250$°K, and the equilibrium conductivity was approximately 31 mho/cm. From these data, $(T_e/T_a-1)_{ideal} = 68(1-K)^2$. Performance curves similar to those of Fig. 6 were computed for this case. Then for several values of K, $(T_e/T_a-1)_{ideal}$ was determined, and from this, J/J_{ideal}, and finally J were computed. A single theoretical curve of J, the current per electrode vs V_y, the terminal voltage, results. It is compared with the data in Fig. 15. Each symbol represents a different pair of electrodes.

Two points should be noted. First, the experimental load line is curved, which strongly suggests nonequilibrium ionization, and the theory gives about the same curvature. Secondly, the magnitude of the predicted current compares very well with the mean of the measured currents for the several electrodes.

Again the theory indicates that this generator operated in the shorted mode, even though H/L was small, because was so large.

C. Other Data

There are other, less quantitative data which support the theory. In his early measurement of the performance of a nonequilibrium generator, Robben[7] obtained only a small fraction of the expected conductivity increase. Furthermore, he observed large potential drops near the electrodes, such as are predicted by the theory. Brederlow, Eustis and Riedmüller,[9] and Chapman[10] report much less than the expected performance from small generator channels operating with noble gases at high Hall parameters.

VI. Concluding Remarks

If we accept the validity of the proposed model for electrode losses in nonequilibrium generators, then we may conclude:

1. For a given generator configuration there is a value of $(T_e/T_a-1)_{ideal}$ above which the generator is subject to Hall current shorts along the electrode walls. The performance of the generator operating in the "shorted" mode is very low unless the segmentation is exceedingly fine.

2. The stability limit moves to lower $(T_e/T_a-1)_{ideal}$ as β_∞ is increased and for this reason the maximum attainable $(T_{e\infty}/T_{a\infty}-1)$ decreases as β_∞ increases, for a given generator design.

3. The stability limit moves to lower $(T_e/T_a-1)_{ideal}$ as H/L is increased, and for this reason the

maximum electron temperature rise attainable in the "normal" mode decreases as H/L is increased.

4. Cooling of the electrode wall moves the stability limit to larger $(T_e/T_a - 1)_{ideal}$, and so increases the maximum $(T_{e\infty}/T_{a\infty} - 1)$

5. In general, for given $(T_e/T_a - 1)_{ideal}$, operation at low β_∞ and large M_∞ is preferable to operation at high β_∞ and low M_∞.

6. The loss due to electrode shorting decreases only very slowly as the generator size is increased. It does not scale according to a surface/volume law.

Certainly the confirmation of the theory by experiment is only very tentative since all of the data appears to be for generators operating in the "shorted" mode. A direct demonstration of the existence of two modes of operation is needed to substantiate the principal results of the theory.

References

1. Klepeis, J. and Rosa, R.J. "Experimental studies of strong Hall effects and V x B induced ionization," 5th Symposium on Engineering Aspects of Magnetohydrodynamics, MIT, April 1964. Also Avco-Everett Research Laboratory Report 177, September 1964.

2. Hurwitz, H. Jr., Kilb, R.W. and Sutton, G.W. "Influence of tensor conductivity on current distribution in a MHD generator," J. Appl. Phys. 32, 205, 1961.

3. Kerrebrock, Jack L. "Segmented electrode losses in MHD generators with nonequilibrium ionization," Avco-Everett Research Laboratory Report 178, April 1964.

4. Lutz, M.A. "Radiant energy loss from a cesium-argon plasma to an infinite enclosure," Avco-Everett Research Report 175, September 1963.

5. Zukoski, E.E., Cool, T.A., and Gibson, E.G. "Experiments concerning nonequilibrium conductivity in a seeded plasma," AIAA Jour. 2, 1410-1417, 1964.

6. Holstein, T. "Imprisonment of resonance radiation in gases, II," Phys. Rev. 83, 1159-1168, 1951.

7. Robben, F. "Nonequilibrium ionization in an MHD generator," Phys. Fluids, 5, 1308-1309, 1962.

8. Croitoru, Z., Bekiarian, A., Graziotti, R. and Pithon, M. "Resultats experimentaux sur les phenomenes d'ionisation hors equilibre dans les generateurs MHD," International Symposium on MHD Electrical Power Generation, Paris, July 1964.

9. Brederlow, G., Eustis, R., and Riedmüller, W. "Measurement of the electron and stagnation temperatures in a linear argon-potassium MHD generator," International Symposium on MHD Electrical Power Generation, Paris, July 1964.

10. Chapman, R.A. Comment made at International Symposium on MHD Electrical Power Generation, Paris, July 1964.

11. Corlis, C.H. and Bozman, W.R. Experimental transition probabilities for spectral lines of seventy elements, NBS Monograph 53, July 1962.

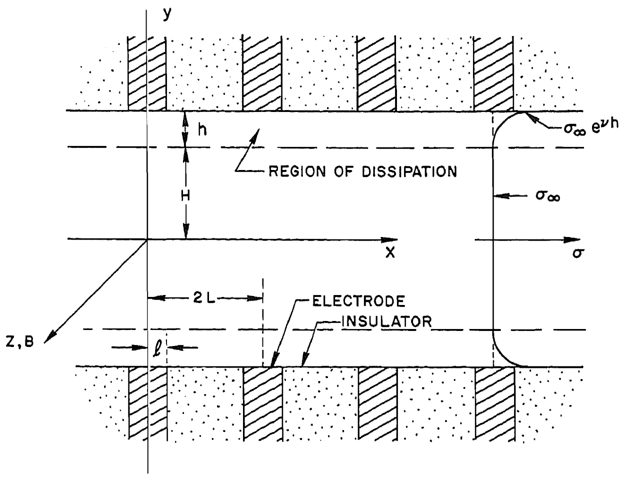

Fig. 1 Schematic diagram of segmented electrode channel showing region of height, h, near electrodes in which the conductivity is larger than the free stream conductivity.

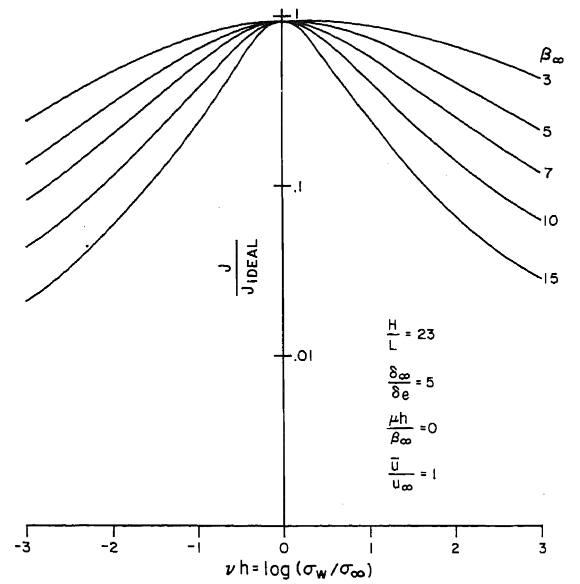

Fig. 2 The ratio of actual to ideal transverse current as a function of the assumed conductivity excess near the electrodes and the Hall parameter. The wall temperature is equal to the gas temperature, while the value of δ_∞/δ_e is characteristic of a least channel dimension of ≈ 1 cm.

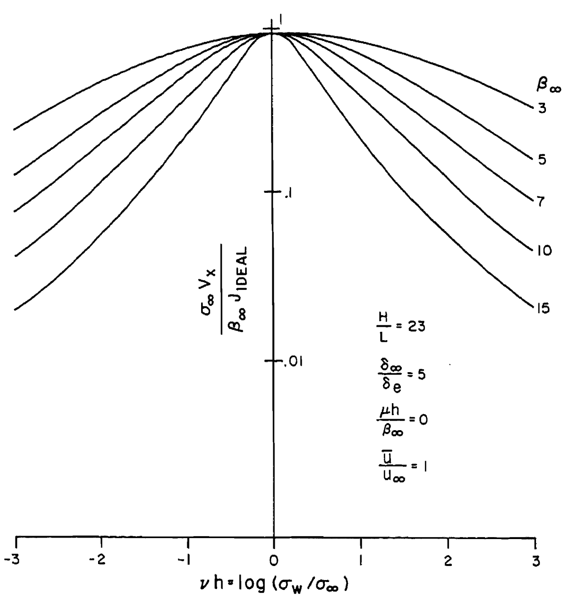

Fig. 3 The ratio of actual to ideal Hall voltage as a function of the assumed conductivity excess near the electrodes and the Hall parameter. The wall temperature is equal to the gas temperature, while the value of δ_∞/δ_e is characteristic of a least channel dimension of ≈ 1 cm.

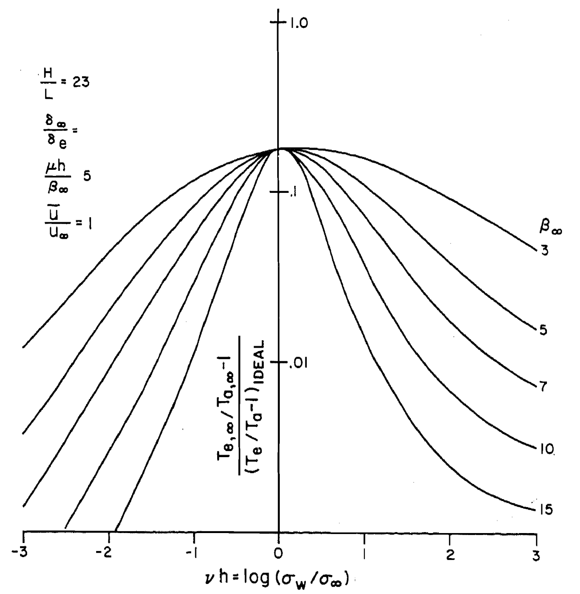

Fig. 4 The ratio of actual to ideal electron temperature rise as a function of the assumed conductivity excess near the electrodes and the Hall parameter. The wall temperature is equal to the gas temperature, while the value of δ_∞/δ_e is characteristic of a least channel dimension of ≈ 1 cm.

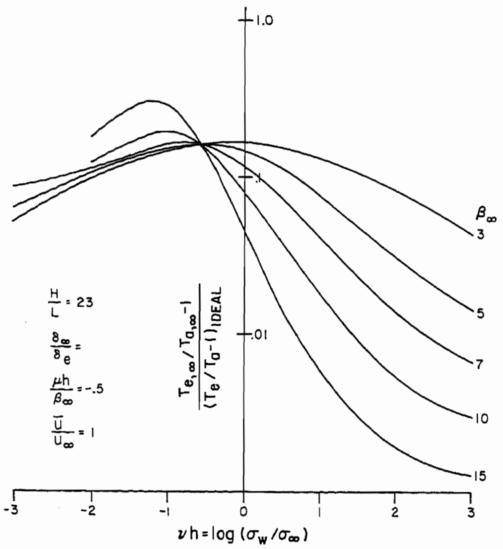

Fig. 5 The ratio of actual to ideal electron temperature rise as a function of the conductivity excess near the electrodes and the Hall parameter. Here the wall temperature is one-half the gas temperature, while the remaining parameters are the same as in Fig. 4.

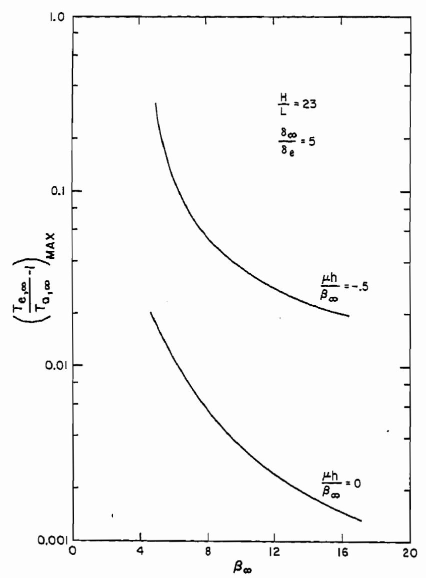

Fig. 7 The maximum electron temperature rise attainable in a generator with H/L = 23 and δ_∞/δ_e = 5 (approximately 1 cm least channel dimension) as a function of Hall parameter and wall temperature ($\mu h/\beta_\infty$). Cooling the electrode wall and lowering β_∞ are both beneficial.

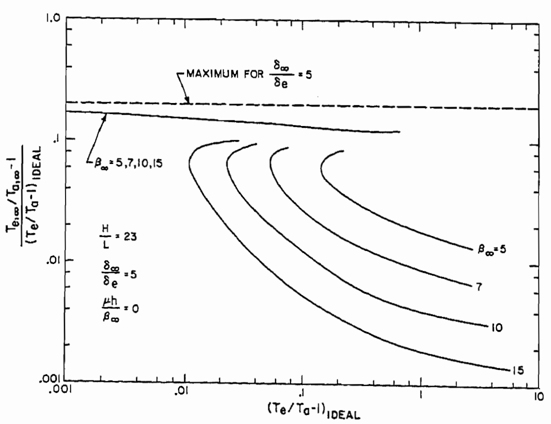

Fig. 10 The ratio of actual to ideal electron temperature rise for the same conditions as given in Fig. 6, except that here the wall temperature equals the gas temperature. Note that the "shorted" mode occurs for lower values of $(T_e/T_a - 1)_{ideal}$ than in Fig. 6.

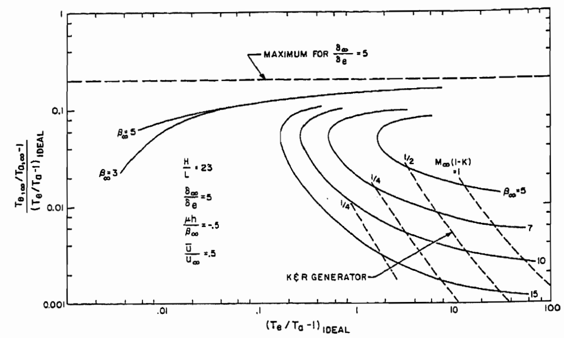

Fig. 6 The ratio of actual to ideal electron temperature rise as a function of the ideal electron temperature rise and the Hall parameter. See Fig. 1 for other notation. Two modes of operation are shown, the "normal" mode at small $(T_e/T_a-1)_{ideal}$ and the "shorted" mode at large $(T_e/T_a-1)_{ideal}$. An approximate operating line for the generator of Klepeis and Rosa[1] is indicated. It operated in the "shorted" mode.

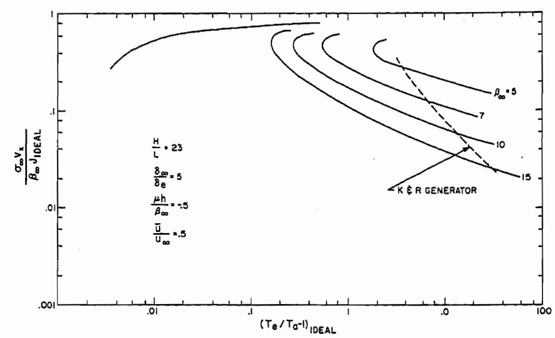

Fig. 8 The ratio of actual to ideal Hall voltages for the case shown in Fig. 6.

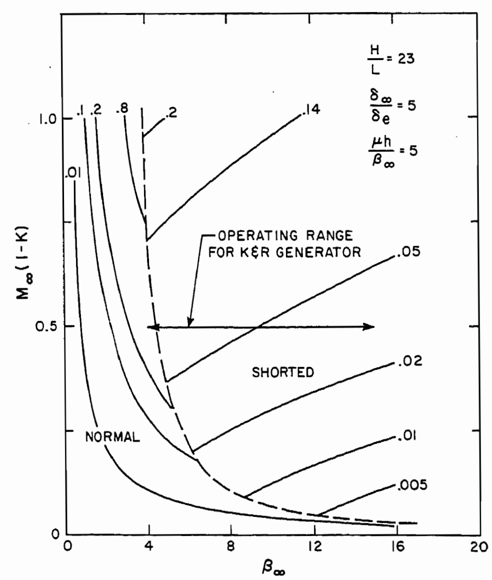

Fig. 9 The fractional electron temperature rise as a function of Mach number, M_∞ loading factor, k, and Hall parameter β_∞ for a channel having H/L = 23, δ_∞/δ_e = 5, and a wall temperature equal to one-half the gas temperature. The dashed line is the boundary between the normal mode and the shorted mode. The operating line of the Klepeis-Rosa generator is indicated by the horizontal arrow.

A3297

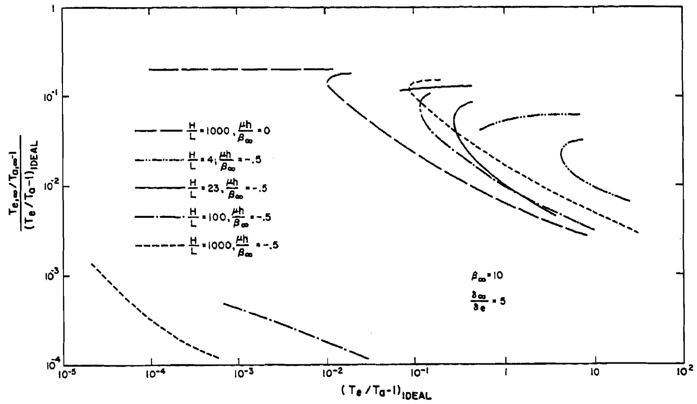

Fig. 11 The ratio of actual to ideal electron temperature rise as a function of the ideal electron temperature rise for revised ratios of channel height to electrode spacing, H/L. For the solid lines the wall temperature is one-half the gas temperature. For the dashed line it is equal to the gas temperature. Note that for H/L > 100, the performance is very low in the "normal" mode because the conductivity is very low near the wall.

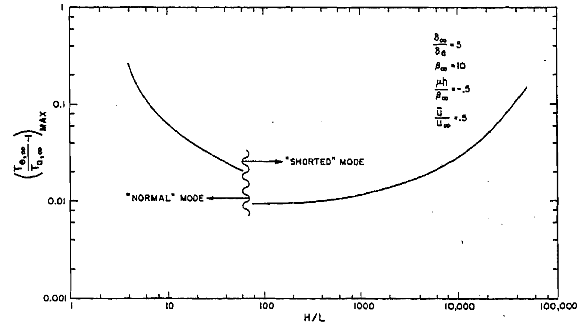

Fig. 12 The maximum attainable electron temperature rise as a function of the ratio of channel height to electrode spacing for a Hall parameter of 10. Rather course segmentation appears to be best for elevating the electron temperature.

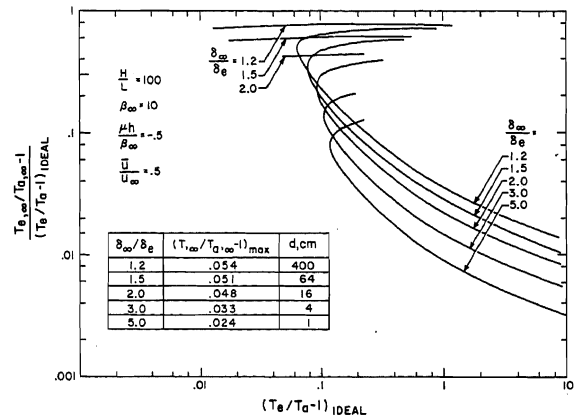

Fig. 13 The effect of generator size on the ratio of actual to ideal electron temperature rise for a Hall parameter of 10. Values of the least channel dimension, d are tabulated with δ_∞/δ_e and the maximum attainable electron temperature rise. It is assumed that the seed concentration is 10^{16} cm^{-3}. Note that the dependence of $(T_{e,\infty}/T_{a,\infty} - 1)$ on d is very weak.

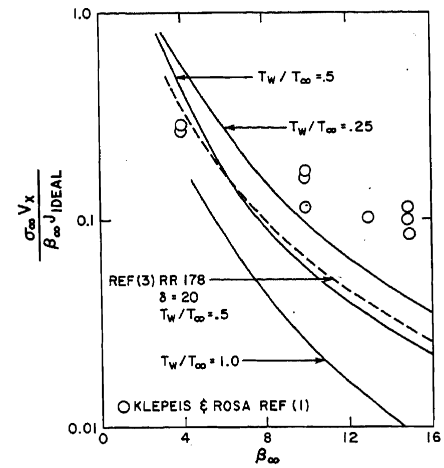

Fig. 14 Comparison of the above theory with the experimental results of Klepeis and Rosa.[1] Theoretical curves are given for three ratios of wall to gas temperature. The theoretical result of Ref. 3 is also given.

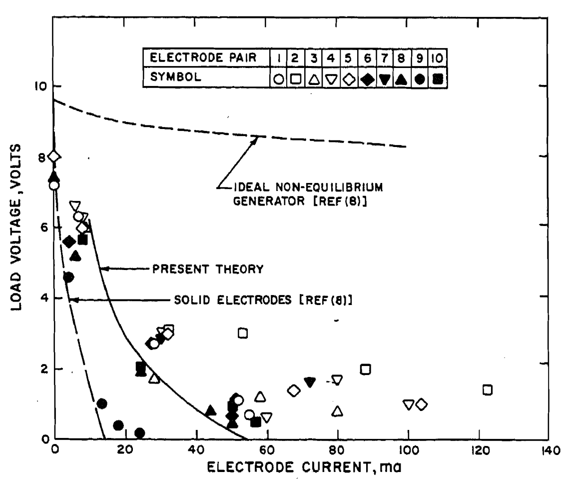

Fig. 15 Comparison of the above theory with the experimental results of Croitoru et al,[8] and with their theoretical results for an ideal generator and for a generator with continuous electrodes. Note that both the data and the theoretical curve show a strong curvature, indicating nonequilibrium ionization, and that the magnitude of the predicted current agrees fairly well with the mean of the electrode currents.